A New View of the Anionic Diene Polymerization Mechanism

A. Z. Niu,[1] *J. Stellbrink,*[1] *J. Allgaier,**[1] *L. Willner,*[1] *D. Richter,*[1] *B. W. Koenig,*[2] *M. Gondorf,*[3] *S. Willbold,*[3] *L. J. Fetters,*[4] *R. P. May*[5]

[1] IFF, FZ Jülich GmbH, 52425 Jülich, Germany
[2] IBI 2, FZ Jülich GmbH, 52425 Jülich and Institut für Physikalische Biologie, Heinrich-Heine-Univ., 40225 Düsseldorf, Germany
[3] ZCH, FZ Jülich GmbH, 52425 Jülich, Germany
[4] School of Chemical and Biomolecular Engineering, Cornell University, Ithaca, NY 14583-5201, USA
[5] Institute Laue-Langevin, 38042 Grenoble, Cedex 9, France

Summary: We investigated the anionic polymerization of butadiene in d-heptane solvent using *tert*-butyl lithium as initiator. Two complementary techniques were used to follow the polymerization processes: ^{1}H NMR and small angle neutron scattering (SANS). The time resolved ^{1}H NMR measurements allowed us to evaluate quantitatively the kinetics of the processes involved. The initiation event commences slowly and then progressively accelerates. This indicates an autocatalytic mechanism. The microstructure of the first monomer units attached is to a high extent 1,2. The disappearance of initiator---at about 10% monomer conversion---signals the onset of the normal ~6% vinyl content of the chain. Small angle neutron scattering was used to study the aggregation behavior of the carbon lithium head groups. It is well known that the polar head groups aggregate and form micellar structures. For dienes in non-polar solvents the textbook mechanism assumes the formation of only tetramers during the propagation reaction. By combining ^{1}H NMR and SANS results we were able to determine quantitatively the aggregation number during all stages of the polymerization. Our measurements show the existence of large-scale structures during the initiation period. The initial degree of aggregation of more than 100 living polymer chains diminished as the polymerization progressed. In addition, even larger, giant structures with $N_{agg} >> 1000$ and $R_g \approx 1000$Å were found.

Keywords: anionic polymerization; kinetics; neutron scattering; NMR; polybutadiene

Introduction

Organolithium compounds self-associate in organic solvents. The aggregation state depends on the solvent and the structure of the compound. It influences significantly the reactivity of organolithium reagents. In hydrocarbon solvents *sec*- and *tert*-butyl lithium form tetramers

 DOI: 10.1002/masy.200451101

whereas *n*-butyl lithium aggregates as hexamers.[1,2] This behavior strongly influences the kinetics of the initiation reaction. The methods used in the past to follow the initiation kinetics were mainly UV spectroscopy[3-5] and to some extent gas chromatic analysis of the hydrolyzed samples taken at different times.[6] It was found that the initiation kinetics of the butyl lithium isomers with styrene and diene monomers are complex. It is first order on monomer concentration and of fractional order in initiator concentration:

$$-d[I]/dt = k_I[BuLi]^{1/n}[M] \quad (1)$$

Depending on initiator, *n* was found to vary between 4 and 6 in benzene and was correlated with the aggregation state of the butyl lithium initiator. It was assumed that there is an equilibrium between the aggregates and the unassociated molecules, the latter ones being the only species initiating the polymerization.[3] Most likely the initiation process is more complex and cross-associated species formed by the reaction of monomer with butyl lithium aggregates could be directly involved.[7,8] In analogy to the short chain initiators, the living polymer chains associate due to aggregation of the carbon lithium active centers was a point of controversy. In earlier studies, the association state of diene based head-groups were a point of controversy.[7-12] Dimers and tetramers were proposed as the association states for completely polymerized systems. The living polymer systems were investigated by concentrated solution viscosity measurements and light scattering.[7-12] Recent publications where small angle neutron scattering (SANS) was used reveal that the aggregation behavior is more complex. All told, the diene based systems can show (depending on the conditions) association degrees ranging from 2 to >100.[13-16]

In this work we analyze the polymerization of butadiene initiated with *tert*-butyl lithium in d-heptane using a combined *in situ* technique of ^{1}H NMR and SANS. ^{1}H NMR allows the simultaneous analysis of the initiation and chain propagation processes. Together, with the SANS results, it was possible to obtain a more detailed picture of the structures involved in the different processes.

Experimental

Solvent and monomer purification techniques have been described.[1,13-16] The polymerization reactions were carried out at 8°C in sealed ^{1}H NMR tubes and SANS quartz cells (Fig. 1). The apparatus equipped with Young® stopcocks was flamed under high vacuum conditions and

transferred into the glove box (MBraun, Unilab®, <0.1 ppm O_2 and <0.1 ppm H_2O). There the initiator solution was filled into the small reactors with a microliter syringe. The Young® stopcocks allowed transfer of the reactors from the glove-box to the vacuum line without contamination with air. Butadiene and d-heptane were distilled from *n*-butyl lithium solutions into small flasks equipped with Young® stopcocks. This allowed the weights to be precisely measured with an analytical balance. Monomer and solvent were then distilled into the reactors quantitatively and the reactors then flame sealed at liquid nitrogen temperature. This was done for the SANS cells by first filling the ingredients into the container below the stopcock (see Fig. 1). After sealing from the vacuum line the contents were warmed to dry ice temperature, poured into the SANS cell and the cell sealed off at -78°C. This procedure was necessary to prevent the cells from cracking during the warm up procedure, of the frozen content, from liquid nitrogen temperature. These procedures allowed precise assay of monomer (10-20 mg) and initiator quantities in the sub μmol range. The monomer concentration was 0.73 mol/L for the ^{1}H -NMR samples and 0.69 mol/L for the SANS samples, the initiator concentration was 8.5×10^{-4} mol/L in all samples.

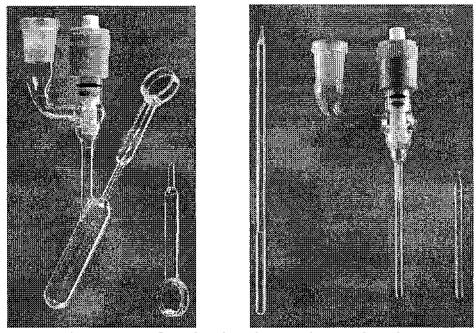

Figure 1. SANS and NMR glassware for the in situ polymerization reactions.

Polymerization reactions were carried out by warming up the samples from liquid nitrogen temperature or dry ice temperature to 8°C within 1 to 3 minutes and keeping the temperature at 8°C±0.7°C for at least two weeks monitoring the polymerization reaction by ^{1}H NMR and SANS. Then the reactors were opened in the glove-box and terminated with degassed methanol. The solutions were filtered, the solvents evaporated and the polymers dried. The samples were

characterized via on-line GPC/light scattering in THF at 30°C. For ^{1}H NMR measurements the reaction mixtures were flame sealed in 4 mm outer diameter ^{1}H NMR tubes (Wilmad, Buena Vista, USA). For measurements in a 5 mm probe the sealed samples were placed into Wilmad 5 mm outer diameter ^{1}H NMR tubes.

Proton NMR spectra were recorded at a Larmor-Frequency of 600.14 MHz on a Bruker DMX600 using a 5 mm TXI probe optimized for proton observation. The free induction decay was recorded immediately after a non-selective 90°-pulse (7 μs) with a dwell time of 111 μs and 32k data points in the time domain. Four transients were added for each spectrum using the CYCLOPS phase cycle to avoid artifacts from quadrature detection. A long pre-scan delay of 300 sec was found to be necessary to ensure complete T_1-relaxation of all signals (strict requirement for quantitative interpretation of integral peak intensity). An exponential window function was applied prior to Fourier transformation and integration of the frequency domain signals.

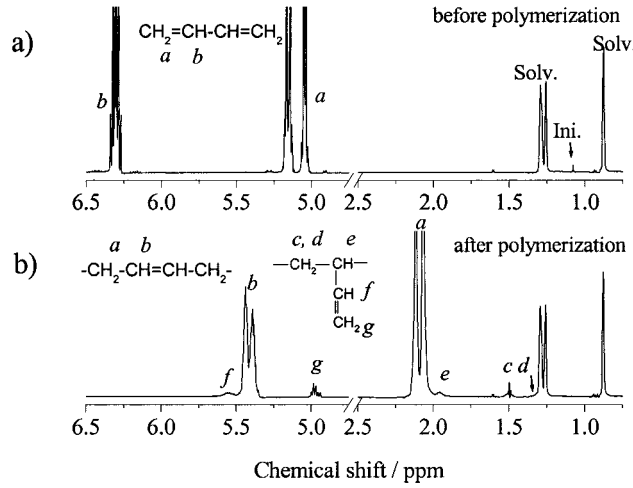

Figure 2. NMR traces of before and after polymerization.

Figures 2a and 2b show typical ^{1}H NMR spectra recorded before and after polymerization, respectively. Signal intensities at different reaction times were compared quantitatively via comparison with the residual proton signal of the solvent n-heptane signal at 0.88 ppm. The molarity of the solvent protons does not change during the polymerization in a sealed sample

tube. The fraction of reacted *tert*-butyl lithium at time t was calculated from the signal intensities at 1.07 ppm of the initial spectrum ($I_{1.07ppm,t=0}$) and the spectrum at time t ($I_{1.07ppm,t}$). Conversion as a function of time, Con.(t), was calculated from the intensities of the monomer signal at ~6.3 ppm ($I_{6.3ppm,t}$) and the polymer signals at ~2.1 ppm ($I_{2.1ppm,t}$, 1,4 structure) and ~1.5 ppm ($I_{1.5ppm,t}$, 1,2 structure) at time t, e.g.:

$$Con.(t) = [P(t)]/([M(t)]+[P(t)]) = (I_{2.1ppm,t}/4+I_{1.5ppm,t})/(I_{6.3ppm,t}/2+I_{2.1ppm,t}/4+I_{1.5ppm,t}). \quad (2)$$

Here, [P(t)] is the polymer repeat unit concentration at time t and [M(t)] is monomer concentration at time t. The polymerization degree $D_p(t)$ was calculated from the signal intensities of the polymer signals at ~2.1 ppm and ~1.5 ppm and the initiator signals at 1.07 ppm as

$$D_p(t) = [P(t)]/([Ini(t=0)]-[Ini(t)]) = (I_{2.1ppm}/4+I_{1.5ppm})/((I_{1.07ppm,\,t=0} - I_{1.07ppm,t})/9) \quad (3)$$

Here, [Ini(t)] is the initiator concentration at time t and [Ini(t= 0)] is initial initiator concentration. Microstructures were calculated from the signal intensities of the polymer signals at ~2.1 ppm and ~1.5 ppm, In all cases the number of protons correlated with the different signals was taken into account.

SANS measurements were performed initially on the KWS2 at FZ Jülich (Germany). These were followed by a series of measurements on D22 at ILL, Grenoble (France). In general, the scattering cross section $\frac{d\Sigma}{d\Omega}$ observed in a SANS experiment from polymers in dilute solution is given by:

$$\frac{d\Sigma}{d\Omega} = \frac{\Delta\rho^2}{N_a}\frac{\phi(1-\phi)}{\left[\frac{1}{V_w P(Q)} + 2A_2\Phi\right]} \quad (4)$$

Here, polymer concentration is given in terms of ϕ which denotes the polymer volume fraction, $P(Q)$ is the form factor of the polymer or the polymer aggregates, V_w the corresponding weight average molecular volume, A_2 the second virial coefficient, and N_a the Avogadro number. $\Delta\rho$ is the scattering contrast defined by:

$$\Delta\rho = \left[\frac{\Sigma b_s}{v_s} - \frac{\Sigma b_{mon}}{v_{mon}}\right] \quad (5)$$

The ratio $\Sigma b_s / v_s$ is the scattering length density of the solvent with b_s the scattering lengths of the

atoms forming the solvent molecule and v_s the corresponding volume. $\Sigma b_{mon}/v_{mon}$ is the corresponding quantity for the repeat unit. To achieve maximum contrast and minimum incoherent background resulting from protonated material, we investigated h-butadiene in d-heptane ($\rho_{h\text{-butadiene}}=4.12\text{x}10^{-9}\text{cm}^{-2}$, $\rho_{d\text{-heptane}} = 6.26\text{x}10^{-10}\text{cm}^{-2}$, $\Delta\rho = 5.85\text{x}10^{-10}\text{cm}^{-2}$). Because all b_i are well defined and tabulated properties of the corresponding nucleus solely, SANS data obtained on an absolute scale can be interpreted quantitatively without any ambiguity. There is no need to determine a contrast parameter experimentally as a function of M_w (such as the *(dn/dc)* used in light scattering experiments).

In general all azimuthally averaged data were corrected for empty cell scattering and then normalized to absolute scattering cross section using a water standard. Contributions due to incoherent background and solvent scattering were subtracted from all data sets before analysis. A useful presentation of the theory and practice of SANS is available from Higgins and Benoit.[18] All experiments were performed at 8°C in order to slow the propagation event. This enables us to obtain time resolved data with good statistics including those at low scattering vectors encountered in the initiation period. This is not trivial since we are starting at $t = 0$ with a monomer solution where scattering intensity is only slightly above that of the solvent.

Combined in situ ^{1}H NMR and SANS Technique

In our study on anionic polymerization, we choose a combination of ^{1}H NMR and small angle neutron scattering (SANS). Using time resolved ^{1}H NMR we obtain quantitative information concerning initiator, monomer, and polymer concentration and polymerisation degree of the single chains as a function of time and conversion ([Ini(t)], [M(t)], [P(t)] and $D_p(t)$), but also structural information on a microscopic level, e.g. the 1,2-to-1,4 ratio. Time resolved SANS on the other hand provides us structural information on a mesoscopic and microscopic length scale, e.g. $R_g(t)$[19] of intermediate aggregates, and quantitative information concerning their M_w. This enables us to cross check kinetics as well as structural data, which makes this combination of experimental techniques especially appealing.

The crucial parameter in a SANS experiment, which determines the spatial resolution, is the scattering vector Q, given by $4\pi\lambda^{-1}\ sin(\Theta/2)$, with θ the scattering angle and λ the neutron wavelength. Q has the dimensions of a reciprocal length and can therefore be regarded as an

"inverse yard stick". For SANS experiments typically performed with different settings, i.e. different sample-to-detector distances and collimation lengths, a Q-range of nearly 2.5 orders of magnitude can be achieved, $1x10^{-3} \leq Q \leq 0.2Å^{-1}$. This corresponds to a spatial resolution $5Å \leq D = 1/Q \leq 1000$ Å. Assuming that the growing chains form only star-like aggregates with a mean functionality N_{agg}, ($N_{agg} = 4$ is predicted by the textbook reaction mechanism), we can derive a quantitative relation for the scattering intensity $I(Q,t)$ observed in a SANS experiment. The scattering intensity as a function of reaction time t and scattering vector Q is then given by:

$$I(Q,t) = \left(\frac{d\Sigma}{d\Omega}\right) \Big/ \left(\frac{\Delta\rho^2}{N_a}\right) = \phi_p(t) \cdot N_{agg}(t) \cdot V_w(t) \cdot P_{star}(Q,t) \qquad (6)$$

Here $P_{star}(Q,t)$ is the form factor of a Gaussian star polymer as given by Benoit[20], which is the only Q-dependent variable in Eq. (6) For simplicity we have neglected the concentration dependence (the second virial coefficient) of $I(Q,t)$. The expected evolution of the scattering intensity calculated $I(Q,t)$ for different conversion between 1% and 100% is illustrated in Fig. 3. One clearly recognises how well suited the chosen SANS setup with respect to Q-resolution is to cover the full polymerization event.

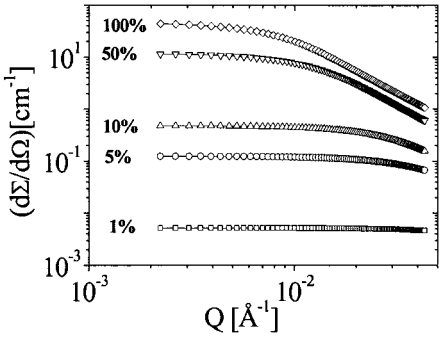

Figure 3. Expected evolution of the SANS scattering pattern with conversion assuming a time independent aggregation state of $N_{agg} = 4$.

In a previous publication,[16] we have shown that all time dependent quantities in Eq. (6) can be reduced to only one parameter, i.e. the number density of reacted monomers $N_p(t)$, which can therefore be calculated from the observed forward scattering $I(Q = 0,t)$. However, this is only valid under two conditions: (1). the number of living chains is time independent and equal to the initiator concentration, i.e. the initiation period has already passed, and (2). all reacted monomers participate in the same type of aggregates with time independent aggregation number. In this case

SANS data alone already give direct access to the reaction kinetics. If we want to extend our studies to the initiation period or if the investigated monomer forms different types of aggregates, we need additional quantitative information to unambiguously interpret our SANS data. The needed information can be independently obtained from time resolved ^{1}H NMR experiments, which gives us directly [Ini(t)], [M(t)], and [P(t)], from which we further can calculate $D_p(t)$ and $M_n(t)$. If we now use these data to analyse our SANS data, we can directly access the aggregation number as a function of time for all phases of the polymerization.

^{1}H NMR Measurements

Careful optimization of experimental conditions was crucial for quantitative interpretation of the ^{1}H NMR spectra. The design of the NMR sample cell, the filling factor of the sealed NMR tube, and the length of the relaxation period required between subsequent scans were found to be critical. ^{1}H NMR spectra were recorded during a first preliminary polymerization attempt with a pre-scan delay of 4 seconds, which turned out to be much too short for complete T_1 relaxation. As a result of this incorrect delay, the overall intensity of the polymer peaks after completion of the polymerization was three times higher than the overall intensity of the monomer peaks of the same sample at the beginning of the reaction. The T_1 relaxation times of the monomer peaks were determined to be (40 ± 5) sec at 8 °C. Spin-lattice relaxation times are significantly shorter for the polymer peaks and decreased with the length of the polymer chain as expected for rapidly tumbling molecules in solution. The most likely explanation for the rather long T_1 values of the solute is solvent deuteration. Nuclear dipole-dipole interaction is a very important relaxation mechanism for protons and the interaction with other nearby protons is particularly efficient due to the extraordinary high gyromagnetic ratio, γ, of protons. Replacing solvent protons with low γ deuterons will increase T_1 of the solute. Paramagnetic impurities, e.g. molecular oxygen, provide another efficient source of T_1 relaxation. However, during the experiments reported here trace amounts of oxygen were carefully removed from the samples to avoid unwanted side reactions. For the quantitative NMR experiments reported in this manuscript a pre-scan delay of 300 sec was used. Further increase of the delay to 1,000 sec did not change the integral intensity of any relevant peak in the spectrum by more than 1%.

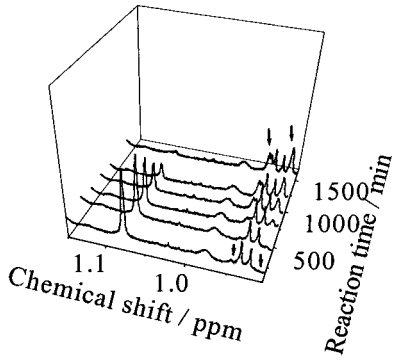

Figure 4. NMR signals of t-butyl lithium and the allyl-lithium head groups.

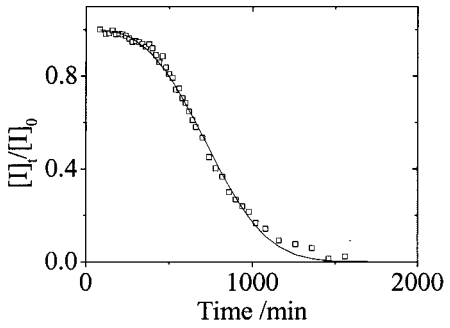

Figure 5. Concentration of reacted initiator normalized by initial initiator concentration $[I]_t/[I]_0$ as a function of time.

In the next polymerization reaction the overall polymer peak intensity was again 20% larger than the initial monomer peak intensity despite the correct pre-scan delay. This time the error could be attributed to the large void volume in the sample tube, which amounted to almost 70% of the tube volume. The void volume contains a substantial fraction of the volatile monomer. For this reason the design of the NMR tube was changed by putting a capillary on top of a 4 mm tube (see Fig. 1). The capillary allows the nearly quantitative filling of the tube while retaining enough distance between the hot glass and the cold liquid during the sealing-off procedure. The short 4 mm sample tube was inserted in a standard length 5 mm outer ^{1}H NMR tube for optimal positioning of the sample in the RF-coil of the probe. This design was used for preparation of all subsequent NMR samples and the overall intensities of the monomer and polymer peaks prior to and after the polymerization, respectively, were found to agree within experimental error. Fig. 4 shows a series of ^{1}H NMR traces during the initiation period at 8°C. With the disappearing initiator signal at 1.07 ppm signals between 0.91 and 0.96 ppm appear, which correspond to the initiated *tert*-butyl lithium. These signals are difficult to analyze quantitatively because of spurious signals appearing in the same ppm range. In Fig. 5 the fraction of reacted *tert*-butyl lithium is plotted against time. The result shows that the initiation reaction starts very slowly and then gradually is accelerated with proceeding initiator consumption. The change of initiation rate with time indicates a kind of

autocatalytic process being involved in the initiation process. Similar results were obtained in the past for the system *sec*-butyl lithium-styrene-benzene using the increase in absorption (334nm) of poly(styryl lithium) to monitor the initiation reaction.[3]

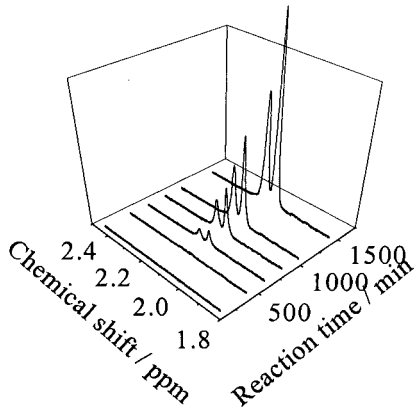

Figure 6. NMR signals of polymer peaks at the beginning of the polymerization reaction.

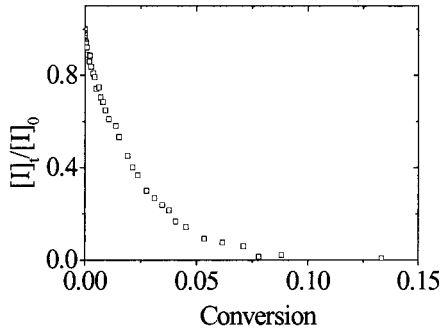

Figure 7. Concentration of residual initiator normalized by initial initiator concentration $[I]_t/[I]_0$ as a function of conversion rate.

Fig. 6 documents the beginning of the propagation reaction. It shows the signals of the 4 aliphatic cis and trans 1,4 protons at approximately ~2.1 ppm. The signals of the protons related to the 1,2 structures at ~1.5 ppm and ~1.9 ppm are hardly visible due to the small concentration. As expected at early reaction times no polymer signal is visible. First after approximately 300 min a hint for the appearance of the signal at ~2.1 ppm is detectable. From the comparison of Fig. 4 and Fig. 6 it can be concluded that before the initiation event is complete the chain propagation has advanced considerably. This is presented in more detail in Fig. 7 where the fraction of reacted *tert*-butyl lithium is plotted against the conversion. Although *tert*-butyl lithium is considered to be a good initiator for diene polymerization in non-polar solvents the initiation step is slower than chain propagation. After consumption of 50 % of the initiator the number average polymerization degree (D_p) of the initiated chains is 15 and after cessation of the initiation step it increases to 75

- 80 which translates to M_n = 4,000 - 4,300. The molecular weight distribution of the final product is not affected because of the 10 times higher overall molecular weight. Furthermore it should be mentioned that the monomer concentration dependence of the propagation rate is first order as it is expected for anionic diene polymerization.[17] From comparison of the polymer signal intensities after completion of the reaction with the initial initiator intensity it was possible to calculate M_n of the polymer. The value found was M_n = 46,400. This is in good agreement with the GPC analysis where M_n was 50,600 and M_w/M_n = 1.04.

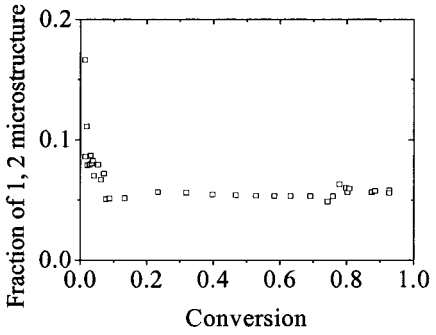

Figure 8. Fraction of 1, 2-microstructure as a function of conversion rate.

^{1}H NMR measurements are useful to investigate the microstructure of polydienes. It is known that in non-polar solvents polymers with mainly 1,4-enchainments are produced. The results obtained during the polymerization process of butadiene are presented in Fig. 8. At very low conversions, the fraction of 1,2-microstructure is between 15 % and 20 %. It then decreases and from 10 % conversion the fraction of 1,2-microstructure is 5-6 % and constant. Similar values as obtained for higher conversion rates of the living process are found for terminated polymers of respective molecular weights. The strong change in microstructure at early polymerization stages indicates that the first monomer units are attached to a high extent in the 1,2-sense. The results shown in Fig. 8 even underestimate the fraction of 1,2-enchainments because in parallel to the initiation event the much quicker chain propagation takes place. This means that smaller chains with a higher 1,2-content exist together with longer chains having a lower 1,2-content and the NMR measurement yields the average value.

SANS Measurements

Fig. 9 shows the temporal evolution of the SANS scattering pattern within the first 60 hours of the polymerisation for butadiene in d-heptane at 8°C. The start of the scattering measurements was synchronized with the beginning of the polymerization event. We collected data initially in 5 minute slices but found that under these experimental conditions the polymerization is quite slow. Within the first 3-5 hours no changes in the scattering pattern were observed. This coincides with ^{1}H NMR experiments, where an induction period of ≈5 hours was observed. Therefore we relaxed our temporal resolution and averaged at each case 4 of these five minutes runs to improve statistics and to align our SANS experiments with the *in situ* ^{1}H NMR; see discussion in ^{1}H NMR section. Furthermore we used the data collected during the first 20 minutes of the polymerisation to correct all further data with this " background run". That is, the scattering intensities shown in Fig. 9 unambiguously result from the polymerization event alone and not from background scattering. The data show exactly the same fingerprint as observed in all previous experiments on butadienyl-lithium. The hallmark is the presence of two characteristic length scales present during all stages of the polymerisation.

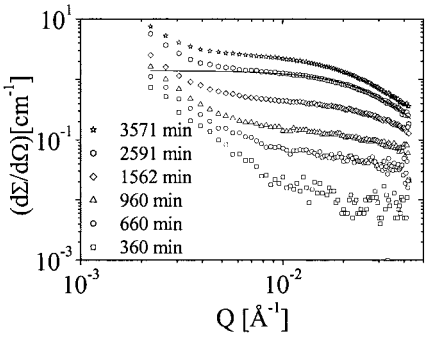

Figure 9. Measured time dependence of the SANS intensity in absolute units vs. scattering vector *Q*. The solid line represents a fit using Eq. (6) and ^{1}H NMR data.

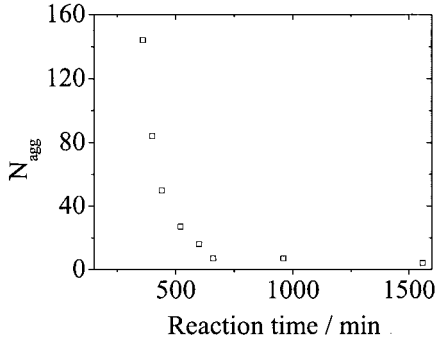

Figure 10. The time dependence of the aggregation number N_{agg} of the smaller aggregates during the early stages of the polymerization.

In the initiation period the scattering pattern is dominated by a pronounced forward scattering at low $Q \leq 10^{-2}$Å^{-1}, which shows a power law decay as $I(Q) \sim Q^{-3}$. This high fractal order is attributed to very dense, large scale aggregates with $R_g \geq 1000$Å and $N_{agg} >> 1000$, probably consisting of mixtures of initiator molecules and initiated chains. As the Q range accessible by SANS is limited, it was not possible to analyse the size of the aggregates more quantitatively. With continuing polymerization, the scattering from these giant structures gets less prominent, but is still visible at the end of the initiation period at about 1500 min. Here D_p is ≈80.

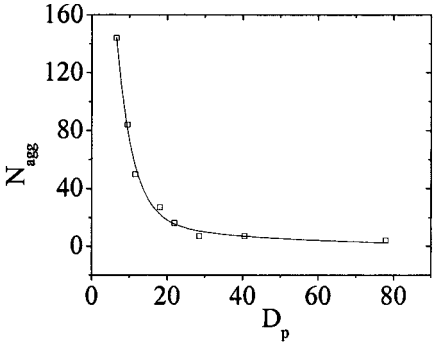

Figure 11. Aggregation number N_{agg} as a function of the polymerization degree D_p. The data fitting result (using the function of the second order exponential decay) yields $N_{agg} = 549.3\exp(-D_p/4.4) + 21.4\exp(-D_p/36.2)$.

The scattering intensity in the higher Q-range increases continuously during the initiation and propagation reaction. It is caused by the smaller aggregates. To analyse them more quantitatively, we applied the following approach. Using D_p of the single chains as a function of time obtained from ^{1}H NMR, we calculated the polymer volume fraction $\Phi(t)$ and an average $V_w(t)$. These results were used for fitting the SANS data to Eq. (6) using a Benoit form factor[20]. This gives direct access to N_{agg} of the aggregates as a function of time, the only adjustable parameter, which determines the scattering intensity. In Fig. 10, aggregation numbers are shown as a function of time. Starting from an average aggregation number of ≈140 in the beginning N_{agg} decays strongly during the initiation period. Fig. 11 shows that the aggregates with higher N_{agg} are composed of oligomeric butadienyllithium. With increasing chain length , N_{agg} gets smaller and levels off at ~4. This value is kept constant during the propagation stage. For the lower aggregation numbers the structure of the aggregates is star-like and is in agreement with the textbook mechanism which assumes tetramers. Experimentally, the limiting value for the dienyl head-group aggregation state is the dimer.[20-22] This is based upon oligomeric poly(butadienyllithium) in the

melt[21] and high molecular weight concentrated solution viscosity measurements (carried out above the crossover concentration, c*, where chain overlap occurs and excluded volume effects are screened out).[22,23] Watanabe and co-workers[24] have concluded that the viscometric method will yield the correct aggregation state for concentrated solutions of high molecular weight dienes. These trends for the variation in aggregation states are in keeping with conclusions from the quantum chemical based calculations of Frischknecht and Milner.[25]

Conclusions

Time resolved ^{1}H NMR measurements allowed us to follow quantitatively the kinetics of anionic polymerization. The initiation reaction is relatively slow compared to the propagation reaction. Moreover, it is already accompanied by a considerable amount of propagation, which results in approximately 10% conversion at the end of the initiation period.

By combining time resolved ^{1}H NMR and SANS experiments we have shown, that there is a complex aggregation behavior in the polymerizing solution. We found at any polymerization stage two families of aggregated species having very different sizes. At the early reaction stages during the initiation period highly aggregated structures with $N_{agg}\approx 100$ and 10Å $\leq R_g \leq$ 100Å are found. As propagation progresses their aggregation number diminishes to a value of 4. These aggregates coexist with even larger, giant structures with $N_{agg} >> 1000$ and $R_g \approx 1000$Å. The relative amount of giant aggregates decreases towards the end of the polymerization. It is not clear if both types of aggregates may consist of mixed aggregates containing both initiator and polymer chains.

[1] M. Morton, L. J. Fetters, *Rubber Chem. Technol.* **1975**, *A12*, 359.
[2] J. Roovers, S. Bywater, *Macromolecules* **1975**, *8*, 251.
[3] S. Bywater, D. J. Worsfold, *J. Organometal. Chem.* **1967**, *10*, 1.
[4] D. J. Worsfold, S. Bywater, *Can. J. Chem.* **1964**, *42*, 2884.
[5] J. Roovers, S. Bywater, *Macromolecules* **1968**, *1*, 328.
[6] H. Hsieh, *J. Polym. Sci.* **1965**, *A3*, 163.
[7] R. N. Young, R. P. Quirk, L. J. Fetters, *Adv. Polym. Sci.* **1984**, *56*, 1.
[8] H. L. Hsieh, R. P. Quirk, *"Anionic Polymerization"*, Marcel Dekker, New York 1996, p.135ff.
[9] D. J. Worsfold, S. Bywater, *Macromolecules* **1972**, *5*, 393.
[10] M. Szwarc, *Adv. Polym. Sci.* **1983**, *49*, 1.
[11] M. Van Beylen, S. Bywater, G. Smets, M. Szwarc, D. J. Worsfold, *Adv. Polym. Sci.* **1988**, *86*, 87.
[12] M. Morton, *"Anionic Polymerization. Principles and Practice"*, Academic Press, New York 1983, p.114.
[13] L. J. Fetters, N. P. Balsara, J. S. Huang, H. S. Jeon, K. Almdal, M. Y. Lin, *Macromolecules* **1995**, *28*, 4996.
[14] J. Stellbrink, L. Willner, O. Jucknischke, D. Richter, P. Lindner, L. J. Fetters, J. S. Huang, *Macromolecules* **1998**, *31*, 4189.
[15] J. Stellbrink, L. Willner, D. Richter, P. Lindner, L. J. Fetters, J. S. Huang, *Macromolecules* **1999**, *32*, 5321.
[16] J. Stellbrink, J. Allgaier, L. Willner, D. Richter, T. Slawecki, L. J. Fetters, *Polymer* **2002**, *43*, 7101.
[17] Ref. 8, p.157ff.
[18] J. S. Higgins and H. C. Benoit, "*Polymers and Neutron Scattering*" Oxford University Press, Oxford 1994.
[19] R_g denotes the radius of gyration.
[20] H. Benoît,. *J. Polym. Sci.*, **1953**, *11*, 507.
[21] H. S. Makowski and M. Lynn, *J. Macromol. Sci.*, **1966**, *1*, 443.
[22] M. Morton and L. J. Fetters, *J. Polym. Sci.*, Part A: **1964**, *2*, 3311.
[23] M. M. Al-Jarrah and R. N. Young, Polymer **1980**, *21*, 112.
[24] H. Watanabe, Y. Oishi, T. Kanaya, H. Kajii and F. Horii, *Macromolecules* **2003**, *36*, 220.
[25] A. L. Frischknecht and S. T. Milner J. Chem. Phys., **2001**, *114*, 1032.